



PCCP

**Exciton Diffusion in Solid Solutions of Luminescent Lanthanide  $\beta$ -Diketonates**

Journal:	<i>Physical Chemistry Chemical Physics</i>
Manuscript ID	CP-ART-09-2020-004889.R1
Article Type:	Paper
Date Submitted by the Author:	28-Nov-2020
Complete List of Authors:	Liu, Mingzhao; Brookhaven National Laboratory, Center for Functional Nanomaterials Yang, Zhanlan; Peking University, Weng, Shifu; College of Chemistry and Molecular Engineering, Peking University, Wu, Jinguang; College of Chemistry and Molecular Engineering, Peking University

SCHOLARONE™  
Manuscripts

Cite this: DOI: 00.0000/xxxxxxxxxx

Exciton Diffusion in Solid Solutions of Luminescent Lanthanide  $\beta$ -Diketonates<sup>†</sup>Mingzhao Liu,<sup>\*a</sup> Zhanlan Yang,<sup>\*b</sup> Shifu Weng<sup>b‡</sup>, and Jinguang Wu<sup>b</sup>Received Date  
Accepted Date

DOI: 00.0000/xxxxxxxxxx

In this Article, a series of luminescent lanthanide  $\beta$ -diketonate solid solutions, in the formula of  $\text{TBAEu}_x\text{M}_{1-x}(\text{TTA})_4$  (TBA = tetrabutylammonium; M = Eu or Gd; TTA = 2-thenoyltrifluoroacetone), are synthesized by co-precipitation. In the solid solutions, the emission efficiency of  $\text{Eu}^{3+}$  is significantly increased with the presence of non-luminescent chelates  $\text{TBALa}(\text{TTA})_4$  and  $\text{TBAGd}(\text{TTA})_4$ . Low temperature luminescent spectroscopy studies indicate that the  $\text{TTA}^-$  ligands in these non-luminescent chelates do emit phosphorescence with long lifetime. However, the ligand phosphorescence is strongly quenched in solid solutions with the luminescent chelate  $\text{TBAEu}(\text{TTA})_4$ , providing a strong evidence for intermolecular energy transfer through the triplet excited states of the ligands. A quantitative analysis of  $\text{Eu}^{3+}$  emission enhancement and  $\text{TTA}^-$  phosphorescence quenching reveals that each  $\text{Eu}^{3+}$  center may receive excitation energy from about 30  $\text{TTA}^-$  ligands, suggesting that the excitation energy has become exciton-like in the solid solutions. Based on the crystallography analysis of  $\text{TBALn}(\text{TTA})_4$ , it is discovered that  $\text{TTA}^-$  ligands in neighboring  $\text{Ln}(\text{TTA})_4^-$  units may form  $\pi$ - $\pi$  stacks with intermolecular distance  $\leq 3.5$  Å, thus enabling efficient triplet exciton diffusion via exchange interaction.

## Introduction

Lanthanide compounds have unique and intriguing optical properties originating from the  $f$ - $f$  electronic transitions.<sup>1-5</sup> The partially-filled  $4f$  orbitals of lanthanide ions are well shielded from the external environment by the O shell ( $n = 5$ ), thus allowing excited  $4f$  states to radiatively relax very efficiently with narrow linewidths at room temperature, despite the relatively low oscillator strengths.<sup>6,7</sup> Lanthanide-based ceramics had been frequently used as phosphors for fluorescent lamps and color displays.<sup>8,9</sup> However, lanthanide ions usually have weak light absorption as the  $f$ - $f$  transitions are Laporte forbidden, making direct optical pumping rather inefficient. Substantially more efficient photoexcitation of lanthanide ions is achieved by forming organometallic complexes with ligands such as carboxylic acids or  $\beta$ -diketones, which usually feature conjugated  $\pi$ -systems for appreciable optical absorption in the UV-blue region.<sup>10</sup> Once optically pumped, the photoexcited ligands may transfer their energy to the lanthanide ions through resonant energy transfer, lead-

ing to significantly more intense emission from the lanthanide ions.<sup>11-13</sup> Numerous lanthanide complexes have been designed and synthesized to maximize their emission quantum yield and stability.<sup>14</sup> In particular, organometallic complexes of  $\text{Eu}^{3+}$  and  $\text{Tb}^{3+}$  have received most attention for their bright luminescence with high color purity, which arises from their relatively simple electronic structures.<sup>13</sup> These unique properties have enabled the luminescent lanthanide complexes for a variety of applications, including time-resolved fluorescent immunoassays, organic light-emitting diodes (OLED), and lasing.<sup>15-20</sup>

Energy transfer from ligand to lanthanide ion cannot proceed if the ligand has narrower energy gap than the center ion. This class includes most complexes of  $\text{La}^{3+}$ ,  $\text{Lu}^{3+}$ , and  $\text{Gd}^{3+}$ , whereas the first two have closed electronic shell and the last has its lowest excited state well into the ultraviolet band. Although these complexes may still emit fluorescence from their ligands, they are generally referred to as non-luminescent due to the absence of characteristic lanthanide ion emissions. Intriguingly, the emission efficiency of luminescent lanthanide complexes may be significantly enhanced by blending with the non-luminescent ones. Commonly referred to as co-luminescence, this effect has been extensively explored to increase the sensitivity of fluorescence-based detection of luminescent lanthanide ions, including  $\text{Sm}^{3+}$ ,  $\text{Eu}^{3+}$ ,  $\text{Tb}^{3+}$ , and  $\text{Dy}^{3+}$ .<sup>21-23</sup> In cases where the lanthanide complexes are dispersed by surfactants as micelles in aqueous solutions, it was reported that the detection sensitivity can be en-

<sup>a</sup> Center for Functional Nanomaterials, Brookhaven National Laboratory, Upton, NY 11973, USA. E-mail: mzliu@bnl.gov

<sup>b</sup> State Key Laboratory of Rare Earth Materials Chemistry and Applications, Peking University, Beijing 100871, China. E-mail: yzl@pku.edu.cn

<sup>†</sup> Electronic Supplementary Information (ESI) available: Elemental analysis, X-ray powder diffraction, and infrared spectra of pure lanthanide chelates and their solid solutions. See DOI: 10.1039/cXCP00000x/

<sup>‡</sup> Deceased.

hanced by over two orders of magnitude.<sup>24,25</sup> Although the effect is typically attributed to intermolecular energy transfer from the non-luminescent complexes to the luminescent ones, a more detailed mechanistic study is difficult due to the disordered nature of micellar/colloidal systems and the vibrational coupling with solvents.

More recently, the co-luminescence effect is studied in solid state systems including bulk powders and thin films, where solvation effect can be excluded and the lanthanide complex molecules take long-range order in 2 or 3 dimensions.<sup>26–30</sup> In these systems, enhancement to lanthanide emission efficiency is similarly observed as the micellar systems. Previously, we reported the co-luminescence effect in solid solutions between  $\text{Eu}(\text{TTA})_3(\text{H}_2\text{O})_2$  and  $\text{Gd}(\text{TTA})_3(\text{H}_2\text{O})_2$  or  $\text{La}(\text{TTA})_3(\text{H}_2\text{O})_2$  (TTA = 2-thenoyltrifluoroacetate) chelates, and found that the  $\text{Gd}^{3+}$  chelate enhances  $\text{Eu}^{3+}$  emission more efficiency than the  $\text{La}^{3+}$  chelate.<sup>28</sup> Based on the finding, we suggested that the enhancement was due to energy transfer between neighboring TTA<sup>−</sup> ligands via their triplet excited state, since photoexcited ligands bound to the paramagnetic  $\text{Gd}^{3+}$  ions would have higher probabilities to land in their triplet states via intersystem crossing. Similar results and conclusions have been reported by Buczek et al, in a very comprehensive studies on thin film solid solutions formed between  $\text{TEALn}(\text{HFA})_4$  chelates (Ln = Sm, Eu, Gd, Tb, and Lu; TEA = tetraethylammonium; HFA = hexafluoroacetylacetonate).<sup>29</sup>

Here we study the co-luminescence in solid solutions formed between  $\text{TBAEu}(\text{TTA})_4$  and  $\text{TBALa}(\text{TTA})_4$  or  $\text{TBAEu}(\text{TTA})_4$  (TBA = tetrabutylammonium). In addition to the observation that  $\text{Eu}^{3+}$  emission efficiency is enhanced by alloying with  $\text{Gd}^{3+}$  and  $\text{La}^{3+}$  chelates, we also discover that the ligand phosphorescence from  $\text{Gd}^{3+}$  and  $\text{La}^{3+}$  chelates is strongly quenched in the solid solutions, providing a concrete evidence for the diffusion of triplet excitons. Comparing with previous studies, a unique advantage of the present system is that the crystal structures of  $\text{TBALn}(\text{TTA})_4$  series have been fully resolved by Criasia et al, with the locations of all atoms determined except for those of hydrogen.<sup>31–33</sup> By analyzing the crystal structure, we reveal that the TTA<sup>−</sup> ligands in neighboring  $\text{Ln}(\text{TTA})_4^-$  ions may form  $\pi$ - $\pi$  stacks with close proximity, which establish a ligand network that greatly facilitates triplet exciton diffusion via exchange interaction.

## Results and discussion

### Structure of the lanthanide chelates

The powdered solid solutions are prepared by co-precipitation of pure  $\text{TBALn}(\text{TTA})_4$  chelates of  $\text{Eu}^{3+}$  and  $\text{La}^{3+}$  or  $\text{Gd}^{3+}$ , to achieve mixing at the molecular level. The formation of chelate rings around  $\text{Ln}^{3+}$  is confirmed by infrared spectroscopy (ESI, Fig. S1), with barely any spectral variation between pure chelates. No change to the infrared spectra is observed after solid solutions are formed, suggesting that the coordination structure remains the same. X-ray powder diffraction patterns of the pure chelates and their solid solutions all appear very similar (ESI, Fig. S2), indicating that the formation of solid solutions has little impact to the lattice. The diffraction patterns are indexed based on the X-ray

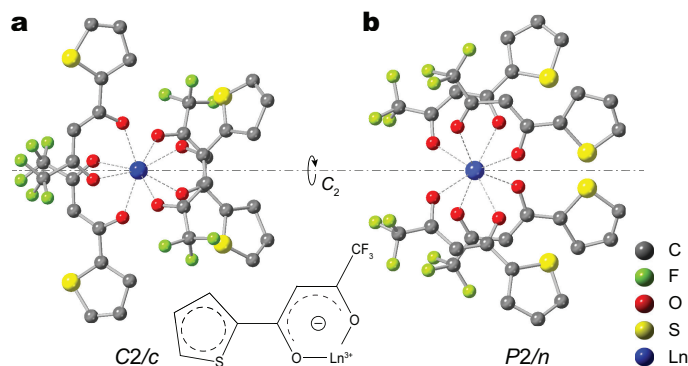


Fig. 1 The molecular structure of  $\text{Ln}(\text{TTA})_4^-$  in the (a)  $C2/c$  and (b)  $P2/n$  isomorphs of  $\text{TBALn}(\text{TTA})_4$ , with hydrogen atoms omitted. Both structures have a  $C_2$  symmetry. Bottom inset shows a simplified chelating structure between TTA<sup>−</sup> and lanthanide ion.

crystallography work by Criasia et al, who studied  $\text{TBALn}(\text{TTA})_4$  single crystals of all lanthanide elements except promethium and concluded that the entire series could take only two isomorphs, respectively in space groups  $C2/c$  and  $P2/n$ .<sup>31</sup> The indexing of our powdered samples reveals that they are all mixtures of the two isomorphs, regardless of them being a pure substance or a solid solution. According to Criasia's results on single crystals,  $C2/c$  is more favored for lighter lanthanides and  $P2/n$  is more favored for heavier ones, despite the absence of a clear-cut boundary with respect to atomic numbers.<sup>31</sup> As shown in Fig. 1, the  $\text{Ln}(\text{TTA})_4^-$  ions have  $C_2$  symmetry and square antiprism coordination shells in both isomorphs. The main difference is that all the thienyl rings are placed to one side of the ion in the  $P2/n$  isomorph but are placed in a more balanced way in the  $C2/c$  isomorph. Therefore, it is very likely that the two isomorphs only have subtle difference in formation energies and a sample prepared by quick precipitation may easily contain both isomorphs.

### Photoluminescence emission from $\text{Eu}^{3+}$

Photoluminescence emission spectrum of  $\text{TBAEu}(\text{TTA})_4$  is collected at room temperature (Fig. 2a), using an excitation wave-

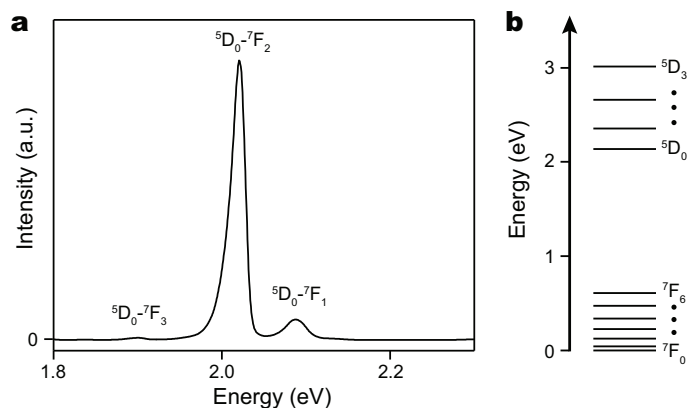


Fig. 2 (a) Room temperature photoluminescence emission spectra of  $\text{TBAEu}(\text{TTA})_4$ . (b) Energy level diagram of  $\text{Eu}^{3+}$ .  ${}^7\text{F}_0$  is the ground state.

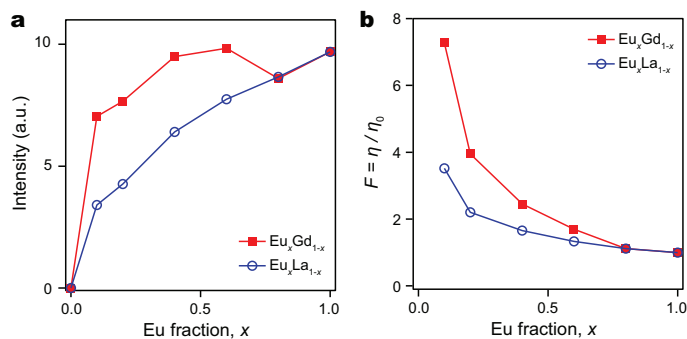


Fig. 3 (a) Dependence of the  ${}^5D_0-{}^7F_2$  emission intensities on the  $\text{Eu}^{3+}$  fraction,  $x$ , for various  $\text{Eu}_x\text{La}_{1-x}$  (blue circle) and  $\text{Eu}_x\text{Gd}_{1-x}$  (red square) solid solutions. (b) Enhancement factor  $F$  for various  $\text{Eu}_x\text{La}_{1-x}$  (blue circle) and  $\text{Eu}_x\text{Gd}_{1-x}$  (red square) solid solutions.

length of 254 nm. According to the energy levels of  $\text{Eu}^{3+}$  (Fig. 2b),<sup>34</sup> the emission is dominated by the hypersensitive  ${}^5D_0-{}^7F_2$  transition (2.02 eV), which is about ten times stronger than the magnetic dipole transition  ${}^5D_0-{}^7F_1$  (2.09 eV). A very weak  ${}^5D_0-{}^7F_3$  transition is observed at 1.90 eV. The spectral profile is characteristic for emissions from  $\text{Eu}^{3+}$  ion occupying a noncentrosymmetric site,<sup>35</sup> which is expected based on the distorted square antiprism coordination sphere of  $\text{Eu}(\text{TTA})_4^-$ .<sup>32,33</sup>

The emission spectra of solid solutions between  $\text{Eu}^{3+}$  and  $\text{La}^{3+}$  (or  $\text{Gd}^{3+}$ ) chelates bear the same profile as the pure  $\text{Eu}^{3+}$  chelate, with similar ratio between the  ${}^5D_0-{}^7F_2$  and  ${}^5D_0-{}^7F_1$  lines. In Fig. 3a, the  ${}^5D_0-{}^7F_2$  emission intensities are plotted against  $\text{Eu}^{3+}$  fractions  $x$  for each  $\text{Eu}_x\text{La}_{1-x}$  and  $\text{Eu}_x\text{Gd}_{1-x}$  solid solutions. The emission intensity is not proportional to the fraction of  $\text{Eu}^{3+}$  in either series but saturates toward higher  $\text{Eu}^{3+}$  fractions. For example, with only 10%  $\text{Eu}^{3+}$ , the  $\text{Eu}_{0.1}\text{Gd}_{0.9}$  solid solution already has emission intensity 73% of the pure  $\text{Eu}^{3+}$  chelate. In another word, the emission efficiency of  $\text{Eu}^{3+}$  is relatively enhanced in the solid solutions, when compared with the pure  $\text{Eu}^{3+}$  chelate. To quantify the emission efficiency of  $\text{Eu}^{3+}$ , the relative emission efficiency  $\eta$  is calculated for each solid solution by normalizing the  ${}^5D_0-{}^7F_2$  emission intensity  $I$  against the  $\text{Eu}^{3+}$  fraction  $x$ , i.e.,  $\eta = I/x$ . We further define an enhancement factor  $F = \eta/\eta_0$  to quantify the enhancement of relative emission efficiency, in which  $\eta_0$  is the relative emission efficiency of  $\text{TBAEu}(\text{TTA})_4^-$ . As shown in Fig. 3b, it is evident that the enhancement is most significant at the lowest fraction of  $\text{Eu}^{3+}$ , and gradually approaches unity towards higher  $\text{Eu}^{3+}$  fractions. In addition, at the same  $\text{Eu}^{3+}$  fraction, solid solution containing  $\text{Gd}^{3+}$  always emits more efficiently than its  $\text{La}^{3+}$  counterpart. The effect is particularly evident at lower  $\text{Eu}^{3+}$  fractions.

The saturation of photoluminescence towards higher  $\text{Eu}^{3+}$  fractions resembles the concentration quenching commonly observed for molecular dye solutions. In concentration quenching, quantum efficiency of emission decreases at elevated emitter concentration due to nonradiative resonant energy transfer between nearby emitters, which eventually degrades excitation energy to heat.<sup>36</sup> However, the phenomenon depicted in Fig. 3 is unlikely accounted for by this mechanism alone. First of all, at low  $\text{Eu}^{3+}$  fractions, the  $\text{Eu}_x\text{Gd}_{1-x}$  solid solution shows significantly higher

emission efficiency than  $\text{Eu}_x\text{La}_{1-x}$ , which cannot be explained by the  $\text{Eu}^{3+}-\text{Eu}^{3+}$  interaction alone. Secondly, due to the low oscillator strength of the  ${}^5D-{}^7F$  transitions of  $\text{Eu}^{3+}$ , Förster resonant energy transfer (FRET) between  $\text{Eu}^{3+}$  ions is very inefficient. According to a joint theoretical and experimental analysis by Tyminski et al, the critical interaction distance  $R_0$ , i.e., the distance at which the donor-acceptor energy transfer rate equals the donor radiative relaxation rate, is merely 2–3 Å for the  $\text{Eu}^{3+}-\text{Eu}^{3+}$  pair.<sup>37</sup> However, the shortest  $\text{Eu}^{3+}-\text{Eu}^{3+}$  distance in the  $\text{TBAEu}(\text{TTA})_4^-$  crystal is about 10 Å. Considering that the FRET rate scales to  $R^{-6}$ , energy transfer between  $\text{Eu}^{3+}$  ions would be negligible in the system we consider. There must be other energy transfer mechanisms holding responsibility for the emission enhancement at lower  $\text{Eu}^{3+}$  fractions, which will inevitably involve the ligands.

### Photoluminescence emission from $\text{TTA}^-$

Detection of the ligand emission becomes possible in the absence of energy transfer between the ligand and the center ion, which holds true for the pure  $\text{La}^{3+}$  and  $\text{Gd}^{3+}$  chelates. Since  $\text{La}^{3+}$  has a closed shell configuration and  $\text{Gd}^{3+}$  has half-filled  $4f$  orbitals ( $4f^7$ ) with its first excited state  ${}^6P_{1/2} \sim 4$  eV above its ground state  ${}^8S_{7/2}$ , photoexcited  $\text{TTA}^-$  ligand cannot relax through resonant energy transfer to either ions. At room temperature, photoluminescence from either chelate remains too weak to be detected. However, broad band photoluminescence emerges over the 2.2–2.5 eV range as these chelates are cooled to 77 K, using an excitation wavelength of 254 nm (Fig. 4a). For both chelates, the emission spectrum features two broad peaks located around 2.46 eV and 2.32 eV. The emission is better characterized as phosphorescence due to its long lifetime, which is  $5.4 \times 10^2$  ms for  $\text{TBALa}(\text{TTA})_4^-$  and  $5.2 \times 10^2$  ms for  $\text{TBAEu}(\text{TTA})_4^-$ . When collecting the emission spectrum, a rotating chopper is applied to intermittently block the excitation beam for a time-delay of about 2 ms, thus filtering out most fast-decaying components. The phosphorescence arises from the radiative relaxation of the ligands' triplet excited states, which are generated through intersystem crossing (ISC) from their singlet excited states. ISC is normally forbidden but becomes possible due to spin-orbital coupling near heavy atoms such as the lanthanide ions. In  $\text{TBAEu}(\text{TTA})_4^-$ , the ISC rate is further enhanced by the spin-spin coupling between the strongly paramagnetic  $\text{Gd}^{3+}$  ( $S = 7/2$ ) and the ligand. Accordingly, phosphorescence intensity from  $\text{TBAEu}(\text{TTA})_4^-$  is about 2.5 times of  $\text{TBALa}(\text{TTA})_4^-$ . In a dilute solution, the triplet energy of  $\text{TTA}^-$  ligand is reported at around 2.52–2.55 eV.<sup>38–40</sup> The slight redshift in our case, by  $\sim 70$  meV, is attributed to  $\pi-\pi$  stacking between neighboring  $\text{TTA}^-$  ligands, which will be discussed further.

Triplet emission from the  $\text{TTA}^-$  ligand is strongly quenched as the  $\text{La}^{3+}$  and  $\text{Gd}^{3+}$  chelates are mixed with the  $\text{Eu}^{3+}$  chelate to form solid solutions (Figures 4b and 4c). The overwhelmingly bright emission of  $\text{Eu}^{3+}$  is largely removed from the phosphorescence spectra with the rotating choppers. However, with the 2 ms delay, the  ${}^5D_0$  emission from  $\text{Eu}^{3+}$  is still clearly visible in the phosphorescence spectra, reflecting the long lifetime of the  ${}^5D_0$

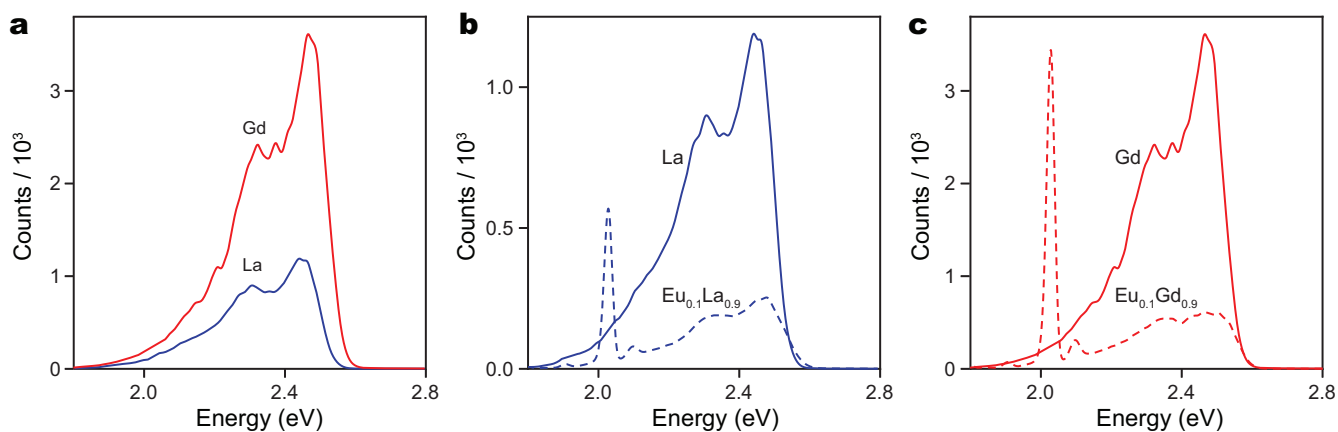


Fig. 4 Phosphorescence spectra of (a) TBALa(TTA)<sub>4</sub> (solid blue) and TBAGd(TTA)<sub>4</sub> (solid red), (b) TBATBAEu<sub>0.1</sub>La<sub>0.9</sub>(TTA)<sub>4</sub> (dashed blue), and (c) TBAEu<sub>0.1</sub>Gd<sub>0.9</sub>(TTA)<sub>4</sub> (dashed blue), collected at 77 K. In panels (b) and (c), the phosphorescence spectra of TBALa(TTA)<sub>4</sub> and TBAGd(TTA)<sub>4</sub> are respectively shown in solid lines for comparison.

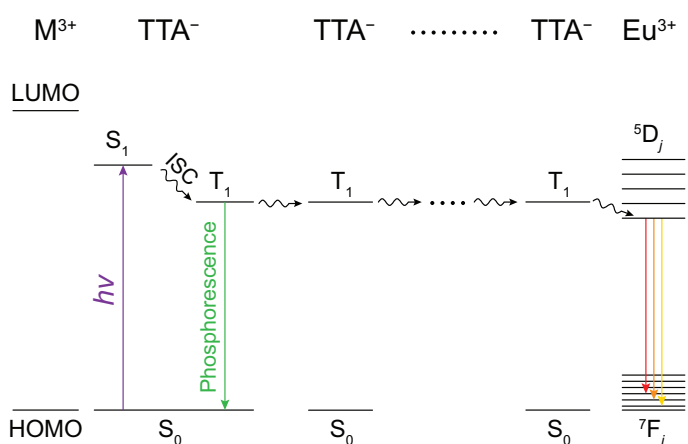


Fig. 5 A simplified Jablonski diagram illustrating the energy transfer path within the TBAEu<sub>x</sub>M<sub>1-x</sub>(TTA)<sub>4</sub> solid solution, which is dominated by the diffusion of triplet excitons (T<sub>1</sub>) in TTA<sup>-</sup> ligands, via exchange interaction. The triplet exciton is generated by the intersystem crossing (ISC) of a singlet exciton (S<sub>1</sub>) and may relax through either phosphorescence emission or energy transfer to an Eu<sup>3+</sup> center.

state ( $\sim 1$  ms).<sup>6</sup> The quenching of ligand phosphorescence is very efficient. At a 10% fraction of Eu<sup>3+</sup>, the phosphorescence intensity of the Eu<sub>0.1</sub>La<sub>0.9</sub> solid solution is only about 1/4 of the pure La<sup>3+</sup> chelate (Fig. 4b). A similar quenching ratio is observed for the Eu<sub>0.1</sub>Gd<sub>0.9</sub> solid solution (Fig. 4c). In solid solutions containing 20% Eu<sup>3+</sup> or more, the quenching becomes so effective that the ligand phosphorescence completely disappears.

### Excitation energy diffusion in the solid solutions

According to Crosby et al, the photoexcited ligand would first relax to a triplet excited state through ISC, before donating its energy to the lanthanide ion for its emission.<sup>11,12</sup> The direct excitation of lanthanide ions is negligible due to the low oscillator strengths of *f-f* transitions. In our case, the TTA<sup>-</sup> ligand has an absorption coefficient at least three orders of magnitude larger than the lanthanide ions, at the excitation wavelength of 254 nm.<sup>41-43</sup> The quenching of triplet emission in the solid solutions suggests

that the photoexcited ligands in La(TTA)<sub>4</sub><sup>-</sup> and Gd(TTA)<sub>4</sub><sup>-</sup> may transfer their energy to the ligands in neighboring Eu(TTA)<sub>4</sub><sup>-</sup>, which in turn contribute to the emission of Eu<sup>3+</sup>. As shown in Figures 4b and 4c, a 10% doping of Eu<sup>3+</sup> quenches the ligand phosphorescence of pure La<sup>3+</sup> or Gd<sup>3+</sup> chelate by about 75%, meaning that on average, one Eu<sup>3+</sup> ion may accept energy from 0.75/0.10 = 7.5 Ln(TTA)<sub>4</sub><sup>-</sup> ions, or 30 TTA<sup>-</sup> ligands. This suggests that the excitation energy becomes delocalized and exciton-like in the solid solutions.

Considering that each Eu<sup>3+</sup> ion in pure TBAEu(TTA)<sub>4</sub> only accepts energy from its own four TTA<sup>-</sup> ligands, we may naively expect that a solid solution containing 10% Eu<sup>3+</sup> has a relative emission efficiency 30/4 = 7.5 times of TBAEu(TTA)<sub>4</sub>. However, such enhancement is observed only for Eu<sub>0.1</sub>Gd<sub>0.9</sub> ( $F = 7.3$ , Fig. 3b). Enhancement for the Eu<sub>0.1</sub>La<sub>0.9</sub> solid solution is significantly lower, with  $F = 3.5$ . The difference strongly suggests that exciton migration within the solid solution is dominated by the diffusion of triplet excitons (T<sub>1</sub>), following a route illustrated in Fig. 5. In this mechanism, the TTA<sup>-</sup> ligands are first optically pumped to the singlet excited state (S<sub>1</sub>). However, only those undergo ISC to T<sub>1</sub> may effectively participate exciton diffusion across neighboring TTA<sup>-</sup> ligands via exchange interaction and eventually lead to the emission of Eu<sup>3+</sup> centers. The validity of this mechanism is based on the observation that TTA<sup>-</sup> in La(TTA)<sub>4</sub><sup>-</sup> has a lower ISC rate than Gd(TTA)<sub>4</sub><sup>-</sup>, which is evident from its weaker phosphorescence emission (Fig. 3a). On the other hand, FRET would make negligible contribution to the triplet exciton diffusion as it involves the dipole-forbidden T<sub>1</sub> – S<sub>0</sub> transitions on both donor and acceptor sides. As such, the Eu<sub>0.1</sub>La<sub>0.9</sub> solid solution would have a lower density of T<sub>1</sub> than Eu<sub>0.1</sub>Gd<sub>0.9</sub>, thus limiting the number of triplet excitons available for each Eu<sup>3+</sup> ion. In an Eu<sub>0.1</sub>M<sub>0.9</sub> solid solution, the density of triplet exciton near each Eu<sup>3+</sup> center may be estimated by

$$\rho_T^M \propto 4\Gamma_{ISC}^{Eu} + 26\Gamma_{ISC}^M, \quad (1)$$

where  $\Gamma_{ISC}^{Eu}$  and  $\Gamma_{ISC}^M$  are respectively the ISC rates of TTA<sup>-</sup> ligands in Eu(TTA)<sub>4</sub><sup>-</sup> and M(TTA)<sub>4</sub><sup>-</sup>. The factors 4 and 26 reflect

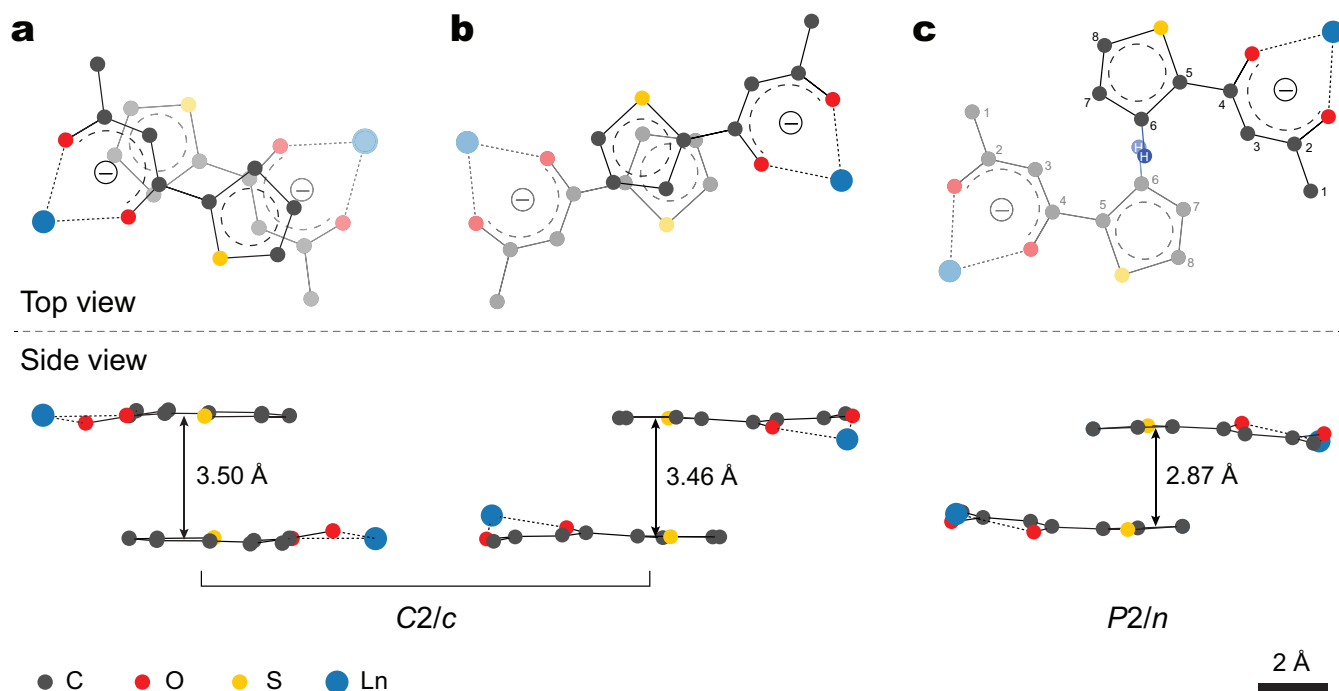


Fig. 6 The  $\pi$ -orbitals of TTA<sup>-</sup> ligands overlap across neighboring Ln(TTA)<sub>4</sub><sup>-</sup> ions. In the C2/c isomorph, two of the four TTA<sup>-</sup> ligands in each Ln(TTA)<sub>4</sub><sup>-</sup> ion are coupled to two Ln(TTA)<sub>4</sub><sup>-</sup> neighbors via mode (a) and the other two are coupled to two more neighbors via mode (b). In the P2/n isomorph, two of the four ligands are coupled to two Ln(TTA)<sub>4</sub><sup>-</sup> neighbors via mode (c), with the nearest  $\pi$ - $\pi$  distance equals 3.4 Å between C6s. Fluorine atoms are omitted for clarity. The locations of hydrogen atoms are not given by X-ray crystallography.<sup>32,33</sup> In panel c, the placement of hydrogen atoms on C6 atoms are based on the typical C-H bond length of 1.09 Å.

that, out of the total 30 TTA<sup>-</sup> ligands that may transfer energy to the Eu<sup>3+</sup> center, 4 of them belong to Eu(TTA)<sub>4</sub><sup>-</sup> and the rest 26 belong to M(TTA)<sub>4</sub><sup>-</sup>. The enhancement factor  $F$  can be derived from Eq. 1 as

$$F = \eta/\eta_0 = \frac{4\Gamma_{\text{ISC}}^{\text{Eu}} + 26\Gamma_{\text{ISC}}^{\text{M}}}{4\Gamma_{\text{ISC}}^{\text{Eu}}} \quad (2)$$

It is therefore clear that  $F$  is dependent upon the ratio of ISC rates  $\Gamma_{\text{ISC}}^{\text{M}}/\Gamma_{\text{ISC}}^{\text{Eu}}$ , which can be determined based on the total quenching of TTA<sup>-</sup> phosphorescence in Eu<sub>*x*</sub>M<sub>1-*x*</sub> solid solutions with  $x \geq 0.2$ . In these solid solutions, all triplet excitons will ultimately transfer their energy to Eu<sup>3+</sup>. As such, the Eu<sup>3+</sup> emission intensity  $I$  may write

$$I = A \left[ x\Gamma_{\text{ISC}}^{\text{Eu}} + (1-x)\Gamma_{\text{ISC}}^{\text{M}} \right], \quad (3)$$

where  $A$  is a proportional factor. The equation establishes a linear correlation between  $I$  and  $x$  for  $x \geq 0.2$ , through which we determine  $\Gamma_{\text{ISC}}^{\text{La}}/\Gamma_{\text{ISC}}^{\text{Eu}} = 0.37$  and  $\Gamma_{\text{ISC}}^{\text{Gd}}/\Gamma_{\text{ISC}}^{\text{Eu}} = 0.84$  via linear regression (ESI, Fig. S3). Using these ratios and Eq. 2, the enhancement factors of Eu<sub>0.1</sub>La<sub>0.9</sub> and Eu<sub>0.1</sub>Gd<sub>0.9</sub> are respectively calculated at 3.4 and 6.5, both excellent fit to experimental values in Fig. 3b. These quantitative results provide strong evidence for the energy transfer mechanism based on triplet exciton diffusion.

The diffusion of triplet excitons requires exchange interaction via electron wavefunction overlapping. According to the crystallography data reported by Criasia, the entire TBALn(TTA)<sub>4</sub> (Ln = lanthanides) series take only two isomorphs, respectively in space groups C2/c and P2/n.<sup>32,33</sup> This is confirmed by our XRD analy-

sis that shows both pure chelates and solid solutions as mixtures of the two isomorphs, with little difference between their XRD patterns (ESI, Fig. S2). Despite the apparent wide separation between neighboring Ln<sup>3+</sup> centers, the TTA<sup>-</sup> ligands in neighboring units remain in close proximity due to the thienyl rings that extend far from the center (Fig. 6). In both the C2/c and the P2/n isomorphs, each TTA<sup>-</sup> ligand is approximately a planar molecule (excluding the fluorine atoms), meaning that the  $\pi$ -systems in the thienyl ring and the  $\beta$ -diketonate chelator are coupled for delocalization of  $\pi$ -electrons across the entire ligand. In the denser C2/c isomorph, each Ln(TTA)<sub>4</sub><sup>-</sup> ion has two nearest Ln(TTA)<sub>4</sub><sup>-</sup> neighbors, with a center-to-center distance of 10 Å. Between each pair of such neighbors, there are one pair of TTA<sup>-</sup> ligands that are overlapping and parallel to each other, with an interfacial distance of only 3.5 Å (Fig. 6a). Considering that the distance is already close to the value in graphite (3.35 Å), a significant  $\pi$ - $\pi$  interaction is expected between the TTA<sup>-</sup> pair through  $\pi$ -orbital overlapping, which greatly facilitates the exchange interaction for triplet exciton diffusion. In addition, each Ln(TTA)<sub>4</sub><sup>-</sup> ion also has two next-nearest Ln(TTA)<sub>4</sub><sup>-</sup> neighbors, with a center-to-center distance of 11 Å. Between such neighbors, there are also one pair of TTA<sup>-</sup> ligands that are parallel to and overlapping each other, with a minimal distance of 3.46 Å (Fig. 6b). Although the second mode has a smaller overlapping that is limited to the thienyl rings, it does enable all four TTA<sup>-</sup> ligands in each Ln(TTA)<sub>4</sub><sup>-</sup> ion to participate energy transfer with neighboring Ln(TTA)<sub>4</sub><sup>-</sup> ions. The  $\pi$ - $\pi$  stacking thus creates a cross-linked network of TTA<sup>-</sup> ligands for efficient triplet exciton diffusion. On the other hand, the P2/n

isomorph has a packing density that is about 3% lower, with different relative orientation between neighboring  $\text{Ln}(\text{TТА})_4^-$  ions. Neighboring  $\text{TТА}^-$  ligands in the  $P2/n$  isomorph thus have significantly smaller overlap. As shown in Fig. 6c, between two neighboring  $\text{Ln}(\text{TТА})_4^-$  ions there are one pair of  $\text{TТА}^-$  ligands that are close and parallel to each other, although true overlapping is only achieved for a pair of hydrogen atoms attached to the thienyl rings. Nevertheless, in this configuration the thienyl rings have a gap of about 3.4 Å, as measured by the nearest distance between the  $\pi$ -backbone atoms (Fig. 6c, the pair of C6 atoms), thus enabling exciton diffusion via exchange interaction.

## Conclusions

In summary, we study the co-luminescence in solid solutions formed between luminescent chelate  $\text{TBA Eu}(\text{TТА})_4$  and non-luminescent chelate  $\text{TBALa}(\text{TТА})_4$  or  $\text{TBA Gd}(\text{TТА})_4$ . In addition to the observation of co-luminescence of  $\text{Eu}^{3+}$  ions, i.e., the emission efficiency of  $\text{Eu}^{3+}$  is enhanced by alloying with  $\text{La}^{3+}$  and  $\text{Gd}^{3+}$  chelates, we also discover that the ligand phosphorescence from  $\text{La}^{3+}$  and  $\text{Gd}^{3+}$  chelates is strongly quenched in the solid solutions. These observations provide a concrete evidence for an intermolecular energy transfer mechanism that is based on the diffusion of triplet excitons, which enables one  $\text{Eu}^{3+}$  center to receive excitons from up to 30  $\text{TТА}^-$  ligands. An analysis of the crystal structure of  $\text{TBALn}(\text{TТА})_4$  indicates that the  $\text{TТА}^-$  ions across neighboring  $\text{Ln}(\text{TТА})_4^-$  ions may achieve close proximity and form  $\pi$ -stacks with intermolecular distance  $\leq 3.5$  Å, thus enabling efficient triplet energy transfer via exchange interaction. The excitation diffusion based on  $\pi$ - $\pi$  interactions is similar as the case observed for  $J$ -aggregate, in which the formation of extensive  $\pi$ -stacks creates delocalized, band-like electronic states.<sup>44</sup> As such, the discovery we report here may open a new avenue to purposefully design luminescent lanthanide chelates to maximize exciton mobility and emission efficiency of the luminescent centers, over solid solutions that are based on either the conventional molecular crystals or the more structurally rigid metal-organic frameworks (MOFs).<sup>45</sup>

## Methods

Lanthanide chloride ( $\text{LnCl}_3$ ) aqueous solutions are fresh prepared by dissolving corresponding lanthanide oxide in 6 M HCl solution while heated. After evaporating excess acid over a vapor bath, each solution is diluted to a desired concentration that is determined by titration against EDTA. Lanthanide oxides  $\text{Eu}_2\text{O}_3$ ,  $\text{La}_2\text{O}_3$ , and  $\text{Gd}_2\text{O}_3$  have purity at least 99.99% and are of spectroscopic grade. Other chemicals, including tetra(*n*-butyl)ammonium iodide (TBAI) and 2-thenoyltrifluoroacetone (HTTA), are of analytical grade and used without further purification.

### Synthesis of $\text{TBALn}(\text{TТА})_4$ ( $\text{Ln} = \text{Eu, La, Gd}$ )

In a typical synthesis, 4 mmol HTTA and 1 mmol TBAI are dissolved in 15 mL ethanol under reflux, after which 4 mmol solid NaOH is introduced to convert the  $\beta$ -diketone HTTA to its enolate form. Under vigorous stirring, 1 mmol of  $\text{LnCl}_3$  aqueous solution

is added dropwise to the solution. After 30 minutes of heating under reflux, the solution is quickly cooled to room temperature, at which point the lanthanide  $\beta$ -diketonate precipitates as a yellow powder. The product is collected by filtration, washed with cold absolute ethanol, and dried at room temperature. The composition of each chelate is obtained from element analysis, which verified their molecular formula as  $\text{TBALn}(\text{TТА})_4$ . Detailed results from the element analysis are listed in the ESI, Table S1.

### Synthesis of luminescent solid solutions

Dry powders of  $\text{TBAEu}(\text{TТА})_4$  and  $\text{TBAM}(\text{TТА})_4$  ( $M = \text{La}$  or  $\text{Gd}$ ) are mixed with desired proportions and dissolved in ethanol under reflux, at the ratio of 15 mL solvent per 1 mmol lanthanide  $\beta$ -diketonate. After cooling to room temperature, the solution is diluted with equal volume of deionized water to precipitate the solid solution quickly and quantitatively. The product is filtered, washed with cold 1:1 ethanol-water solution, and dried at room temperature. The final solid solution preserves the same  $\text{Eu}:\text{M}$  ratio as the value used for the preparation, which is confirmed by inductively coupled plasma atomic emission spectroscopy (ICP-AES). Detailed results from the ICP-AES analysis are listed in the ESI, Table S2.

### Emission spectroscopy characterizations

Photoluminescence spectroscopy and lifetime studies are performed with a Hitachi F-4500 fluorescence spectrophotometer, using monochromized 254 nm radiation from a xenon lamp as the excitation source. On both excitation and emission sides, monochromator slits are set for a spectral bandwidth of 2.5 nm. For room temperature measurements, 0.1 g dry powder of each sample is filled into a plastic dish of 10 mm diameter and 1 mm depth. The dish is held at the intersection of the excitation and detection light paths with an inclination of 45° to each direction. For low temperature phosphorescence measurements, each sample is placed in a quartz tube and cooled to 77 K by liquid nitrogen, with a rotating chopper that intermittently blocks the excitation beam to collect the emission at a time-delay of about 2 ms.

### Conflicts of interest

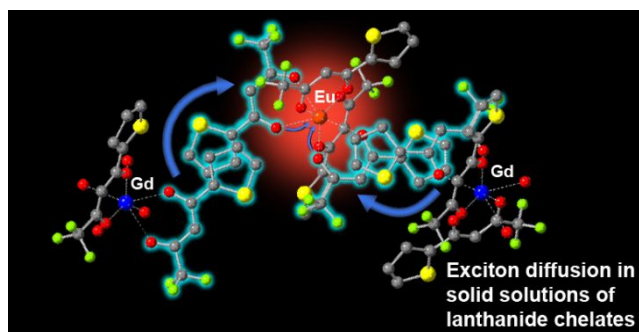
There are no conflicts to declare.

### Acknowledgements

Z.L.Y., S.F.W., and J.G.W. acknowledge financial support from the State Key Projects for Fundamental Research of MOST (G1998061311), National Natural Science Foundation of China (200230005), and CURE. The primary research contribution of M.Z.L. was carried out while at Peking University supported as noted above, and M.Z.L. now acknowledges support from the Center for Functional Nanomaterials, which is a U.S. DOE Office of Science User Facility, at Brookhaven National Laboratory under Contract No. DE-SC0012704. The authors thank Prof. C. H. Yan and Prof. L. D. Sun for their help on the low temperature emission spectroscopy.

## Notes and references

- 1 W. F. Krupke, *Phys. Rev.*, 1966, **145**, 325–337.
- 2 F. Wang and X. G. Liu, *Chem. Soc. Rev.*, 2009, **38**, 976–989.
- 3 S. Heer, K. Kompe, H. U. Gudel and M. Haase, *Adv. Mater.*, 2004, **16**, 2102–2105.
- 4 Q. L. Dai, M. E. Foley, C. J. Breshike, A. Lita and G. F. Strouse, *J. Am. Chem. Soc.*, 2011, **133**, 15475–15486.
- 5 K. Binnemans, *Chem. Rev.*, 2009, **109**, 4283–4374.
- 6 M. H. V. Werts, R. T. F. Jukes and J. W. Verhoeven, *Phys. Chem. Chem. Phys.*, 2002, **4**, 1542–1548.
- 7 A. Døssing, *Eur. J. Inorg. Chem.*, 2005, **2005**, 1425–1434.
- 8 T. Jüstel, H. Nikol and C. Ronda, *Angew. Chem. Int. Ed.*, 1998, **37**, 3084–3103.
- 9 W. C. Nieuwpoort and G. Blasse, *Solid State Comm.*, 1966, **4**, 227–229.
- 10 S. I. Weissman, *J. Chem. Phys.*, 1942, **10**, 214–217.
- 11 R. E. Whan and G. A. Crosby, *J. Mol. Spectrosc.*, 1962, **8**, 315–327.
- 12 J. J. Freeman and G. A. Crosby, *J. Phys. Chem.*, 1963, **67**, 2717–2723.
- 13 W. M. Watson, R. P. Zerger, J. T. Yardley and G. D. Stucky, *Inorg. Chem.*, 1975, **14**, 2675–2680.
- 14 L. Armelao, S. Quici, F. Barigelletti, G. Accorsi, G. Bottaro, M. Cavazzini and E. Tondello, *Coord. Chem. Rev.*, 2010, **254**, 487–505.
- 15 I. Hemmilä and V. Laitala, *J. Fluoresc.*, 2005, **15**, 529 – 542.
- 16 A. K. Hagan and T. Zuchner, *Anal. Bioanal. Chem.*, 2011, **400**, 2847 – 2864.
- 17 G.-L. Law, K.-L. Wong, H.-L. Tam, K.-W. Cheah and W.-T. Wong, *Inorg. Chem.*, 2009, **48**, 10492–10494.
- 18 F. Zinna, M. Pasini, F. Galeotti, C. Botta, L. Di Bari and U. Giovanella, *Adv. Funct. Mater.*, 2017, **27**, 1603719.
- 19 K. Kuriki, Y. Koike and Y. Okamoto, *Chem. Rev.*, 2002, **102**, 2347–2356.
- 20 H. Liang, Q. J. Zhang, Z. Q. Zheng, H. Ming, Z. C. Li, J. Xu, B. Chen and H. Zhao, *Opt. Lett.*, 2004, **29**, 477–479.
- 21 Y.-Y. Xu, I. A. Hemmilä and T. N.-E. Lövgren, *Analyst*, 1992, **117**, 1061–1069.
- 22 S. Lis, M. Elbanowski, B. Mąkowska and Z. Hnatejko, *J. Photochem. Photobiol. A*, 2002, **150**, 233 – 247.
- 23 V. L. Ermolaev and S. E. B., *Russ. Chem. Rev.*, 2012, **81**, 769–789.
- 24 Y. Ci and Z. Lan, *Anal. Chem.*, 1989, **61**, 1063–1069.
- 25 Y.-Y. Xu and I. A. Hemmilä, *Anal. Chim. Acta*, 1992, **256**, 9 – 16.
- 26 G.-L. Zhong and K.-Z. Yang, *Langmuir*, 1998, **14**, 5502–5506.
- 27 Y. Y., S. Q. and Z. G., *J. Mol. Struct.*, 2000, **525**, 47 – 52.
- 28 M. Z. Liu, Z. L. Yang, L. Zhang, S. F. Weng and J. G. Wu, *Acta Phys.-Chim. Sin.*, 2001, **17**, 797–801.
- 29 K. Buczek and M. Karbowski, *J. Lumin.*, 2013, **136**, 130 – 140.
- 30 A. Y. Grishko, V. V. Utochnikova, A. A. Averin, A. V. Mironov and N. P. Kuzmina, *Eur. J. Inorg. Chem.*, 2015, **2015**, 1660–1664.
- 31 R. T. Criasias and M. Cefola, *J. Inorg. Nucl. Chem.*, 1975, **37**, 1814–1815.
- 32 R. T. Criasias, *Inorg. Chim. Acta*, 1987, **133**, 195–200.
- 33 R. T. Criasias, *Inorg. Chim. Acta*, 1987, **133**, 189–193.
- 34 G. H. Dieke, H. M. Crosswhite and H. Crosswhite, *Spectra and energy levels of rare earth ions in crystals*, Interscience Publishers, New York, 1968, pp. xi, 401 p.
- 35 K. Binnemans, *Coord. Chem. Rev.*, 2015, **295**, 1–45.
- 36 A. G. Tweet, W. D. Bellamy and G. L. Gaines, *J. Chem. Phys.*, 1964, **41**, 2068–2077.
- 37 J. K. Tyminski, C. M. Lawson and R. C. Powell, *J. Chem. Phys.*, 1982, **77**, 4318–4325.
- 38 W. R. Dawson, J. L. Kropp and M. W. Windsor, *J. Chem. Phys.*, 1966, **45**, 2410–2418.
- 39 S. Sato and M. Wada, *Bull. Chem. Soc. Jpn.*, 1970, **43**, 1955–1962.
- 40 W.-S. Lo, W.-T. Wong and G.-L. Law, *RSC Adv.*, 2016, **6**, 74100–74109.
- 41 A. Strasser and A. Vogler, *Inorg. Chim. Acta*, 2004, **357**, 2345 – 2348.
- 42 S. RAM, O. P. LAMBA and H. D. BIST, *Pramana*, 1984, **23**, 59–68.
- 43 K. Binnemans, C. Görller-Walrand and J. Adam, *Chem. Phys. Lett.*, 1997, **280**, 333 – 338.
- 44 T. Brixner, R. Hildner, J. Köhler, C. Lambert and F. Würthner, *Adv. Energy Mater.*, 2017, **7**, 1700236.
- 45 J. Rocha, L. D. Carlos, F. A. A. Paz and D. Ananias, *Chem. Soc. Rev.*, 2011, **40**, 926–940.



Photoluminescence from Eu(III)  $\beta$ -diketonate is enhanced in solid solutions with non-luminescent lanthanide  $\beta$ -diketonates. The effect is attributed to triplet exciton diffusion through the formation of  $\pi$ - $\pi$  stacks between neighboring ligands.